

## Low-temperature oxidation effects on the morphological and structural properties of hexagonal Zn nanodisks

R. López<sup>a,\*</sup>, E. Viguera-Santiago<sup>b</sup>, S. Hernández-López<sup>b</sup>, P. Acuña<sup>c</sup>, A. Argueta-Vega<sup>d</sup>,  
N. Colín-Becerril<sup>d</sup>, G. Villa-Sánchez<sup>a</sup>, and J. Rosales-Dávalos<sup>a</sup>

<sup>a</sup>*Tecnológico de Estudios Superiores de Jocotitlán (TESJo),  
Carretera Toluca-Atlaconulco km 44.8, Ejido de San Juan y San Agustín, Jocotitlán, Edo. México, México.*

<sup>b</sup>*Laboratorio de Investigación y Desarrollo de Materiales Avanzados (LIDMA),  
Facultad de Química, Universidad Autónoma del Estado de México,  
Paseo Colón esquina Paseo Tollocan, Toluca Estado de México, México.*

<sup>c</sup>*Estudiante del programa de Doctorado en Ciencia de Materiales de la Universidad Autónoma del Estado de México,  
Paseo Colón esq. Paseo Tollocan, Toluca, México.*

<sup>d</sup>*Estudiante del programa de Ingeniería Mecatrónica. Tecnológico de Estudios,  
Superiores de Jocotitlán (TESJo).*

*Carretera Toluca-Atlaconulco km 44.8, Ejido de San Juan y San Agustín,  
Jocotitlán, Edo. México, México.*

*\*e-mail: lorr810813@gmail.com*

Received 3 October 2016; accepted 28 March 2017

Ambient-atmosphere oxidation in the temperature range of 90-450°C was performed over Zn films composed by well-faceted hexagonal nanodisks, which were deposited by thermal evaporation. Morphological and structural properties of oxidized Zn nanodisks were studied by scanning electron microscopy, transmission electron microscopy, energy dispersive spectroscopy, X-ray diffraction, and Raman scattering measurements. It was found that Zn nanodisks keep its original shape only when they are annealed at 90 or 150°C. Smooth oxidation occurred only on the rectangular faces of Zn nanodisks heated at 150°C. Thermal oxidation at 250°C favored growth of ZnO nanoneedles over the surface of the Zn nanodisks. Hexagonal-shape of Zn nanodisks was transformed completely into a complex morphology composed by different shaped particles, with further increase in oxidation temperature to 450°C.

*Keywords:* Zn nanodisks; thermal oxidation; ZnO nanoneedles.

PACS: 81.07-b; 81.65.Mq; 81.07.Bc

### 1. Introduction

Nanostructured ZnO is a functional material with interesting physical properties for several applications such as dye-sensitized solar cells, excitonic lasing, biosensors, transistors, gas sensors, among others [1,2]. For example, in gas sensing, high surface-to-volume ratio is a key parameter that improves sensitivity of the ZnO-based sensor [3]. Although ZnO nanostructures can be fabricated with a rich variety of morphologies, using simple and low cost techniques, in many cases nanostructured ZnO exhibits a very complicated morphology, composed by a mixed combination of nanoparticles with different shape and sizes [4]. Historically, one advantage of thermal processes is that they improve crystalline quality of materials. For example, it is known that ZnO with high structural quality can be prepared efficiently by thermal oxidation of Zn [5]. However, at the view-point of nanoscale, the main disadvantage of heating nanostructured Zn is that the use of oxidation temperatures near its melting point favors growth and agglomeration, which in most cases modifies the nano-sized particle distribution, changes their morphology, and increase the size of the nanoparticles [6]. These non-expected effects have been also observed when nanostructures are annealed [7,8].

Therefore, study of thermal treatments performed to nanoparticles or nanostructures is interesting not only in terms of oxidation or improve crystallization, but also to keep their novel properties. For example, although bulk Zn is a metal, it has been found that Zn nanoplates exhibit both semi-conducting properties and efficient photoluminescence from ultraviolet to red, at room temperature [9]. It has also been reported that thermal oxidation at temperatures in the range of 100- 500°C performed to Zn nanospheres, allows to tune the photoluminescent properties [10]. In the present work, a systematic study of thermal oxidation in the range of 90 to 450°C was performed to evaluate oxidation temperature dependence with morphology and structure of well-faceted Zn nanodisks.

### 2. Material and methods

Zn nanodisks were prepared by the thermal evaporation in a high-vacuum evaporation deposition system (Intercovamex TE12). Glass slices (20 × 20 mm) and aluminum foils were used as substrates and fixed on a substrate holder, 10 cm above a molybdenum boat filled with 250 mg of Zn powders (98% of purity). Substrate temperature and deposition time are shown in Fig. 1. Once the vacuum pressure of the

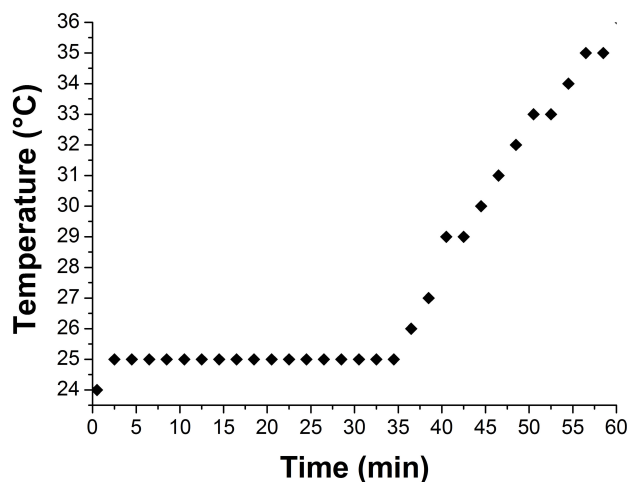


FIGURE 1. Substrate temperature and deposition time during deposition of Zn nanodisks. Since substrate was placed 10 cm above from the evaporation zone (molybdenum boat), the substrate was mainly heated by radiation, reaching a maximum temperature of 36°C.

chamber was pumped to  $2 \times 10^{-6}$  Torr, a molybdenum boat was heated by raising the electrical current with a rate of 3.3 A/min, reaching a current of 124 A and holding it there for 60 min, with no carrier gas introduced. It was observed a slightly and instantly increase to  $7 \times 10^{-6}$  Torr in the chamber pressure due to evaporation of Zn when electrical current was increased to 124 A. Zn nanodisks were heated in ambient-atmosphere at temperatures between the range of 90-450°, for three hours in a horizontal tube furnace (Lindberg company). The products were characterized by scanning electron microscopy (SEM, JEOL JSM-6510LV) and by Field-Emission SEM (FESEM, JSM-7401F). The structural analysis was carried out using a high-resolution transmission electron microscope (HRTEM, JEM-2200FS) with an acceleration voltage of 200 kV, and an X-ray diffractometer (XRD, Bruker D8 Advances) with a radiation of  $\text{CuK}\alpha$  (1.541 Å). The lattice spacing was measured by using ImageJ software. Raman spectra were recorded with a HR-800 (Jobin-Yvon-Horiba) LabRaman analyzer equipped with a He-Ne laser (632.817 nm).

### 3. Results and discussion

#### 3.1. Zn nanodisks

Figure 2 shows XRD pattern of products obtained by thermal evaporation. It reveals peaks at  $2\theta = 36.27^\circ$ ,  $38.97^\circ$ ,  $43.15^\circ$ , which correspond to the (002), (100), and (101) lattice planes, respectively, of the hexagonal Zn structure (space group P63/mmc; JCPDS No. 04-0831). Some workers have previously reported that in temperatures of below 200°C, Zn still keep pure without an oxide layer on its surface [9,10]. As shown in Fig. 1, while deposition of Zn nanodisks was performed, the substrate reached a maximum temperature of about 36°C. The inert state of Zn near room-temperature

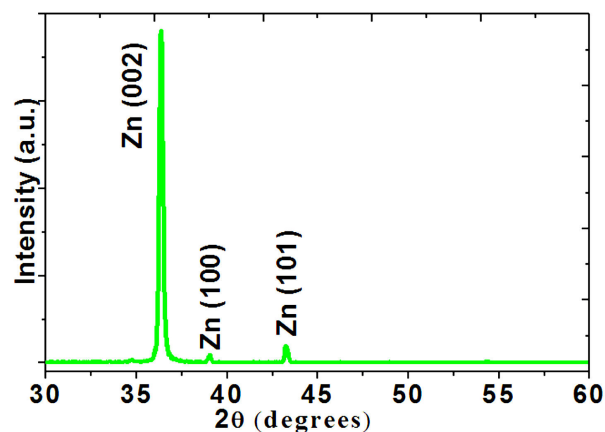


FIGURE 2. XRD pattern of Zn nanodisks synthesized by thermal evaporation at a vacuum-pressure of  $10^{-6}$  Torr.

makes difficult surface oxidation. Thus, additional peaks corresponding to lattice of ZnO were not observed in the XRD pattern.

Morphology of Zn deposited by thermal evaporation was characterized by SEM. Fig. 3a shows that the substrate is covered by a high number of polygonal-shaped Zn particles. The cross-sectional view shows that the thick of the layer is about 2 micrometers (Fig. 3b). In order to clarify the morphological aspects of each individual Zn particle, some powders were collected from surface of the pyrex-bell jar where a low density of deposited material was found. The Shape of the observed Zn particles is described as a section of a regular hexagonal prism (Fig. 3c). EDS spectrum shown in Fig. 3d. only exhibits peaks of Zn, without detectable O. The carbon signal was probably originated by the carbon support-film where the Zn products were placed during the SEM measurements.

The structure of Zn nanodisks was also characterized by HRTEM. In Fig. 4a, the six-fold symmetry of the single particle corroborates that the Zn nanodisks exhibit a well-faceted hexagonal geometry. The nanodisk is partially transparent to the electron beam, which suggest the nanodisks have a low thickness. The d-spacing of the nanodisk has a measured value of 0.23 nm (Fig. 4b), which agrees with (100) planes of Zn (SAED pattern at inset of Fig. 4b). Formation mechanism of Zn nanodisks has been associated to supersaturation of Zn vapor [11]. Since the vacuum-pressure was  $10^{-6}$  Torr and the substrate was kept near room-temperature (as showed in Fig. 1), high supersaturation conditions can be assumed near the substrate and a vapor-solid mechanism could explain the formation of well-faceted hexagonal Zn nanodisks.

#### 3.2. Oxidation of Zn nanodisks

Thermal treatments at 90, 150, 250, and 450°C in ambient-atmosphere were performed to follow the evolution of structural and morphological properties during oxidation of the Zn nanodisks. It has been reported that the hexagonal shape of Zn nanodisks is transformed when they are heated at temper-

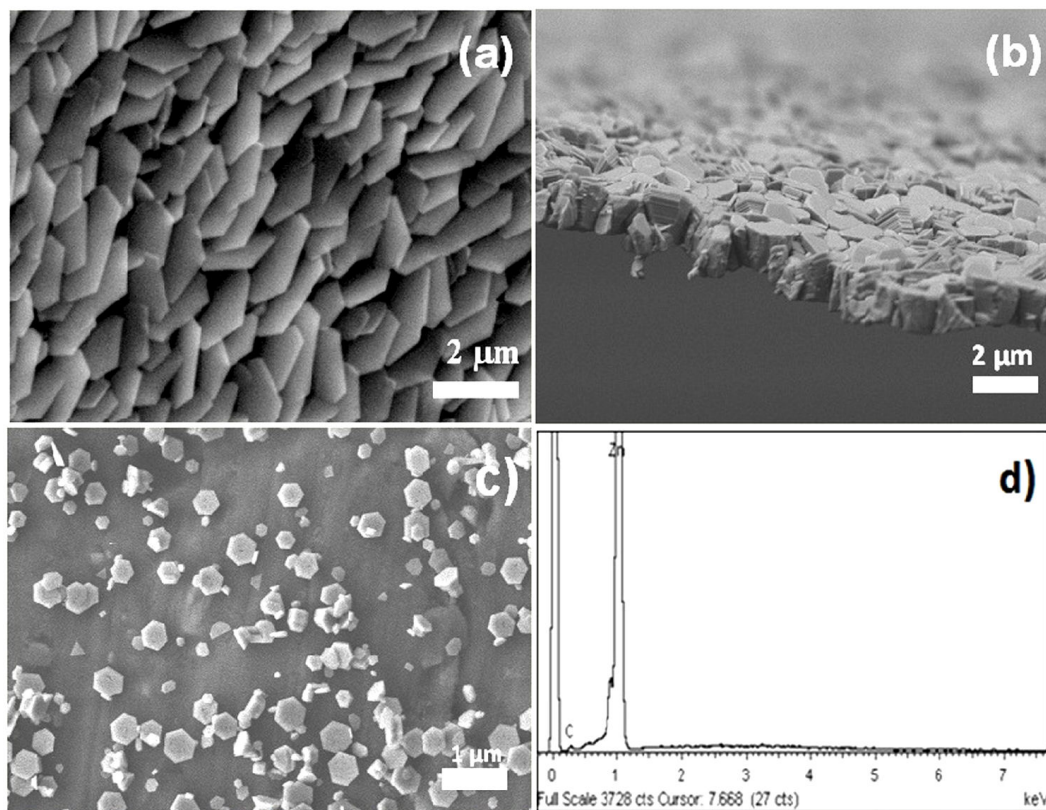


FIGURE 3. SEM images of Zn nanodisks deposited by thermal evaporation: a) material deposited 10 cm above the molybdenum boat (evaporation zone), b) cross-sectional view of the Zn nanodisks layer, c) Zn nanodisks collected from the pyrex bell jar, and d) EDS spectrum of Zn nanodisks.

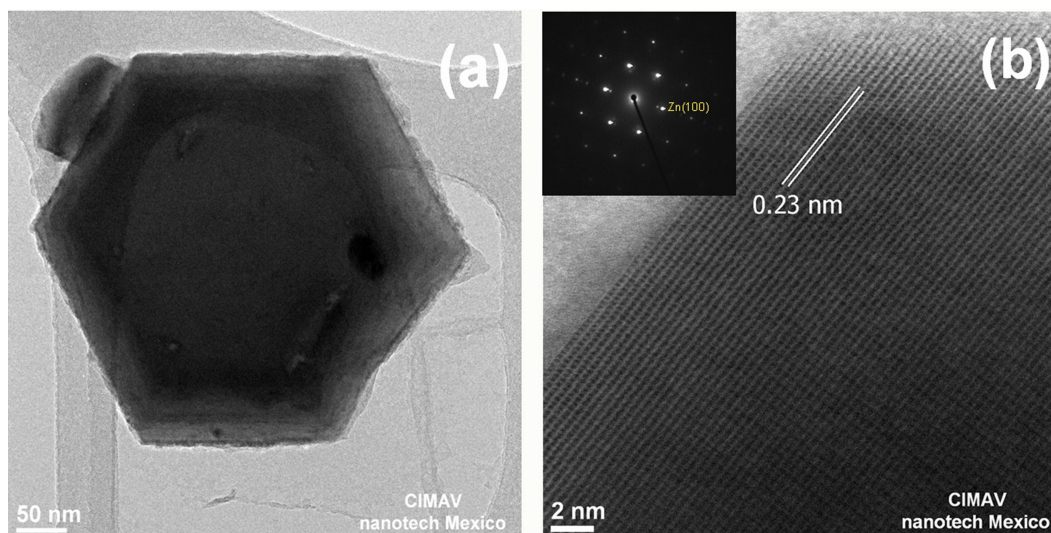


FIGURE 4. TEM measurements: a) image of a single hexagonal nanodisk, b) HRTEM image where the observed d-spacing corresponds to (100) planes of hexagonal Zn lattice (inset at the upper left corner).

atures above 100°C [12]. With the aim of confirm such assumption, the Zn nanodisks were first annealed at 90°C. From Fig. 5a it is observed that the particles keep its hexagonal shape. However, in contrast with as-deposited Zn nanodisks, its EDS spectrum includes a weak oxygen peak

(Fig. 5b). SEM image of Zn nanodisks annealed at 150°C is shown in Fig. 5c. Morphology of such particles is similar to that of the Zn nanodisks heated at 90°C. However, high-magnification SEM image (Fig. 5d) shows that sheet-like particles were formed at the edge of each nanodisk. EDS

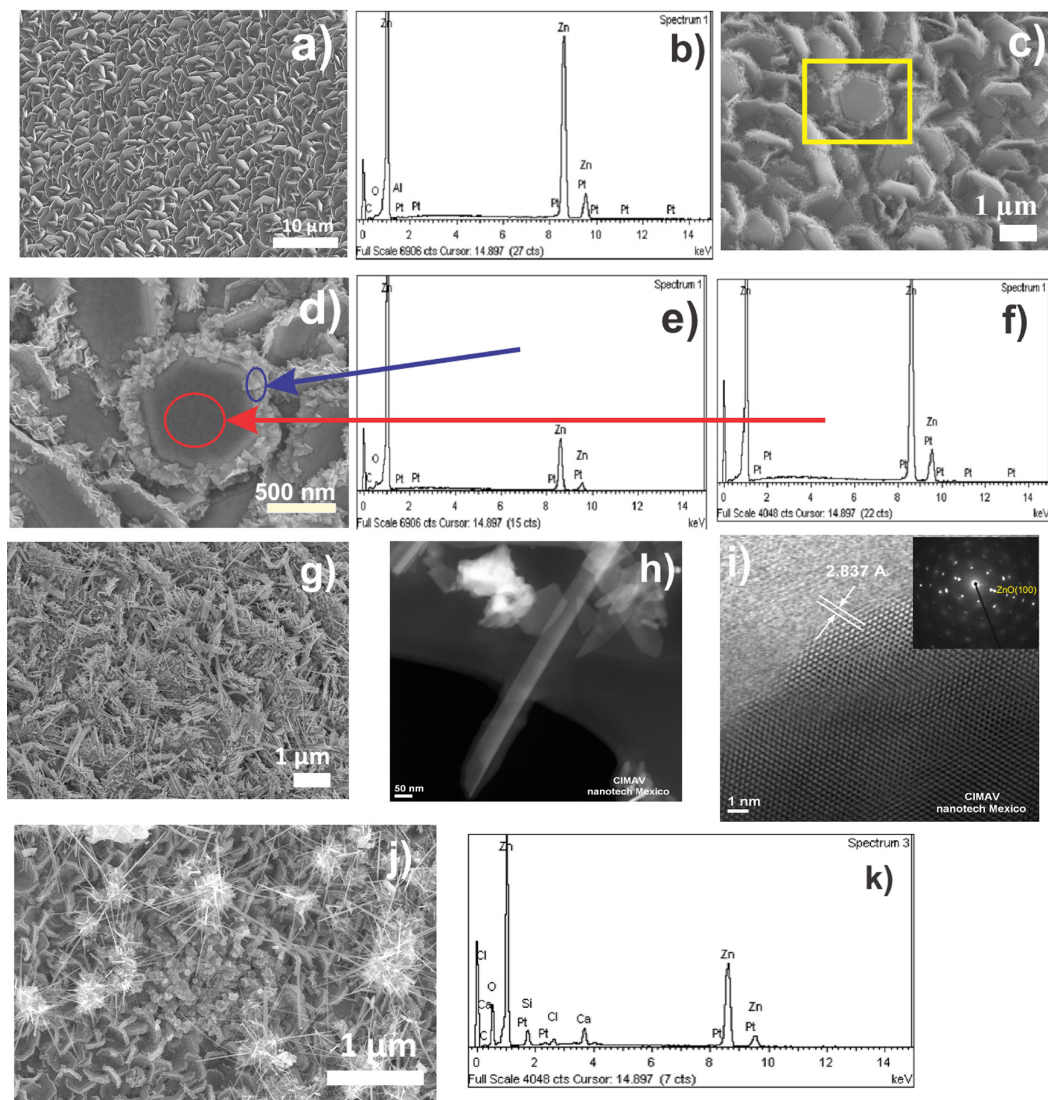


FIGURE 5. Electron images of Zn nanodisks heated at temperatures of : 90°C (a) SEM image, (b) EDS spectrum; 150°C (c) SEM image, (d) high-magnification image of Fig 5c, (e) EDS spectrum measured from edge of a nanodisk, (f) EDS spectrum from center of a nanodisk; 250°C (g) SEM image, (h) TEM image of a nanoneedle, (i) HRTEM image of a nanoneedle and its corresponding SAED pattern (inset at the upper right corner); 450°C (j) SEM image, and (k) EDS spectrum.

measured from the edge of a nanodisk (Fig. 5e, marked by blue arrow). shows Zn, C, and O peaks. Although EDS qualitatively shows only elements, the oxygen peak could be evidence of the formation of ZnO at the edge of the nanodisk since EDS performed at the center of it (Fig. 5f, marked by red arrow) shows only Zn peaks. This oxidation behavior at 250°C could be explained in terms of surface energy. According to the hexagonal structure, the basal planes are (0001) and the prism planes are (1 0 -1 0), (1 -1 0 0), and (0 1 -1 0). Since oxidation rates on different crystal surfaces are different, surfaces with lower energy tend to be most stable and may resist being oxidized, while surfaces with higher energy will quickly oxidize. Since the prism planes for hexagonal structure exhibit higher surface energy than the basal planes, it is expected that such faces are firstly oxidized [13]. Thus, oxygen was detected only when EDS was performed at the

edges of the nanodisks, which corresponds to elemental analysis on the prism planes. It is important to note that the oxidation behavior observed for Zn nanodisk is different than other Zn nanoparticles. For example, some works have previously shown that oxidation is uniform over the entire surface of a Zn nanosphere [10]. SEM image of Zn nanodisks annealed at 250°C is shown in Fig. 5g. The structure is observed to be composed by needle-like particles, which grew over the surface of the nanodisks. TEM image of a single needle is shown in Fig. 5h. The image shows that the diameter of a nanoneedle is below 100 nm. HRTEM image of a nanoneedle is shown in Fig. 5i. The lattice fringes with d-spacing of 0.28 nm match with (100) planes of ZnO (SAED pattern at the inset of Fig. 5i), which confirms the formation of single crystalline ZnO nanoneedles. Further thermal treatments at temperatures of 350 and 400°C were performed to the Zn

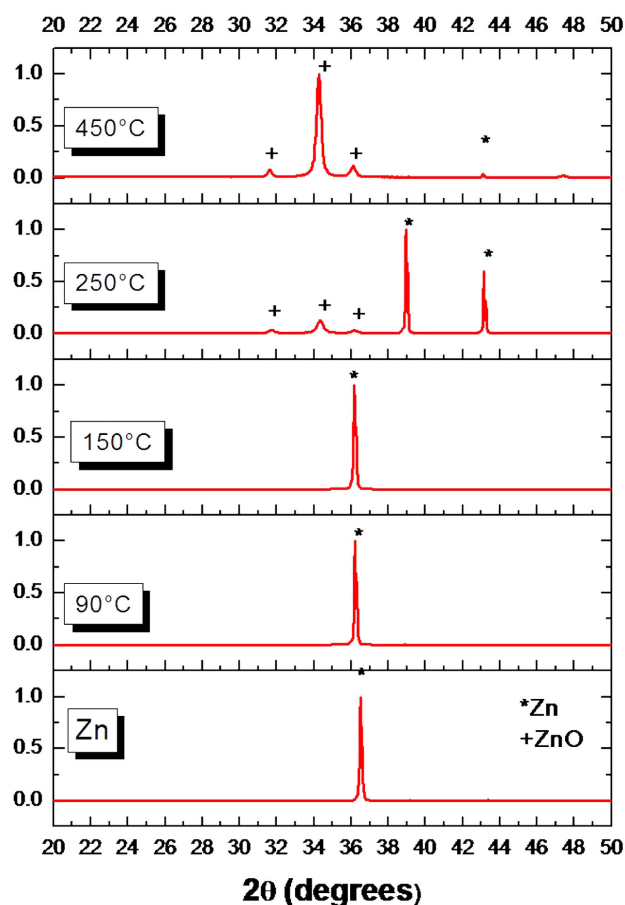


FIGURE 6. XRD patterns of hexagonal Zn nanodisks thermal treated in ambient-atmosphere at temperatures between 90 to 450°C. XRD pattern of as-prepared Zn was included for comparative purpose.

nanodisks (not shown here). However, the observed structure showed similar morphological characteristics. Transformation of the nanoneedle-nanodisk structure was observed by thermal treatment at 450°C ( $\sim 30^\circ\text{C}$  above melting point of Zn)(Fig. 5j). The structure is observed to be composed by a very complex morphology with different shaped-particles such as urchins, needles, and spheres. Corresponding EDS spectrum of nanodisks annealed at 450°C show that Zn and oxygen peaks are the main elements (Fig. 5k).

XRD technique was used to identify crystalline phase of nanodisks thermal treated in the range of 90 to 450°C (Fig. 6). XRD patterns of nanodisks annealed at 90 and 150°C were indexed to the hexagonal structure of Zn (JCPDS No. 04-0831), and no peaks related to ZnO were found. Although a weak signal of oxygen was found in EDS spectra for the aforementioned samples, specially for that where oxygen was found at the edge of nanodisks, there are some considerations that should be take into account. For example, EDS is a local probe and XRD provides global information and only detects crystalline phases. Also, some additional effects and measurement parameters such as organic contamination of sample, acceleration voltage, line used for quantification, among others, should be considered in matching XRD with

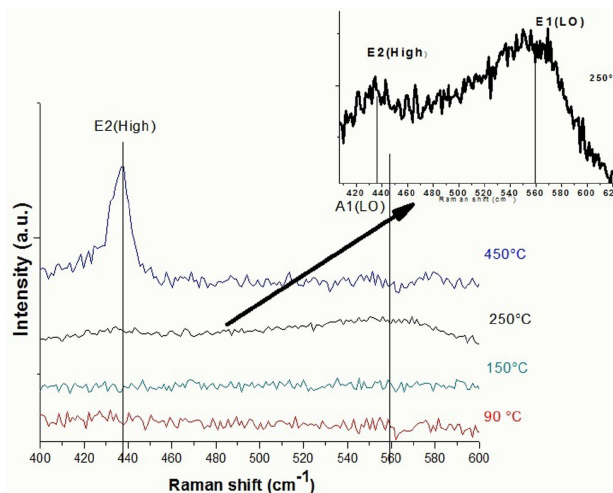


FIGURE 7. Raman spectra of Zn nanodisks thermally oxidized at 90, 150, 250, and 450°C.

EDS results. XRD pattern of nanodisks annealed at 250°C shows some additional weak peaks to the already Zn peaks. These peaks were found at  $2\theta = 31.66, 34.34$  and  $36.15^\circ$ , corresponding to the planes (100), (002) and (101) of the wurtzite structure of ZnO (JCPDS card no. 36-1451). Although the morphology was observed to be mainly composed by ZnO nanoneedles (Fig. 5g), presence of sharp and intense Zn peaks suggests that the metal is still dominant in the sample deposited at 250°C. Finally, as was expected, XRD pattern of nanodisks annealed at 450°C shows that Zn was almost transformed into ZnO and only weak Zn peak at  $43.04^\circ$  is still observed.

Raman scattering measurements were performed to provide complementary information about crystalline structure of Zn nanodisks thermal treated in the temperature range of 90-450°C (Fig. 7). Although EDS spectrum showed that ZnO was formed at the edges of nanodisks heated at 150°C, ZnO was not detected within the detection limit of Raman of nanodisks heated at 90 and 150°C, as was also observed in XRD results. Raman spectrum of Zn nanodisks oxidized at 250°C shows only a broad band centered at approximately  $560\text{ cm}^{-1}$ . This peak is attributed to the  $E_1(\text{LO})$  mode, which is caused by defects such as oxygen vacancies [14]. A close-up view (inset of Fig. 7) of Raman spectrum of Zn nanodisks oxidized at 250°C displays a line at  $438\text{ cm}^{-1}$ , corresponding to the high  $E_2$ -mode of the non-polar optical phonons, generally attributed to the bulk ZnO. As characteristic peak of ZnO, the  $E_2$ -mode at  $438\text{ cm}^{-1}$  is usually very intense. From comparative intensity between the high  $E_2$ -mode and the  $E_1(\text{LO})$ , it was expected that peak at  $438\text{ cm}^{-1}$  should be stronger than peak at  $560\text{ cm}^{-1}$ . This unexpected effect in which the peak at  $560\text{ cm}^{-1}$  showed higher intensity than peak at  $438\text{ cm}^{-1}$  could be related with the excess of Zn since the sample oxidized at 250°C was not completely oxidized. Raman spectrum for sample oxidized at 450°C shows only the Raman-line at  $438\text{ cm}^{-1}$ . The absence of the  $E_1(\text{LO})$  mode at  $560\text{ cm}^{-1}$  indicates that this sample is of high qual-

ity because that mode is associated with lattice defects. However, XRD results showed that the structure of the deposited material was not completely oxidized at 450°C.

#### 4. Conclusion

The effect of thermal oxidation in a low-temperature range on properties of hexagonal Zn nanodisks was studied. It was found that morphological and structural characteristics of Zn nanodisks can be controlled in temperatures of oxidation around and below 150°C. Further temperature increase leads to gradual transformation from well-faceted Zn nan-

odisks to a complex morphology, composed by ZnO particles with non-controlled sizes and morphologies.

#### Acknowledgments

This work was supported by Universidad Autónoma del Estado de México grand 1025/2014RIFC. We wish to thank Laboratorio Nacional de Nanotecnología (CIMAV-Chihuahua, México) and Carlos E. Ornelas for HRTEM assistance. Also thanks to Dr. Gustavo Lopez Tellez from Centro Conjunto de Investigación en Química Sustentable UAEM-UNAM for SEM measurements.

- 
1. Xiao Wei Sun and Yi Yang, *ZnO nanostructures and Their Applications*, CRC Press, Boca Raton, FL 33487-2742.
  2. A. Djuricic, X. Chen, Y. Leung, A. Ching, *J. Mater Chem* **22** (2012) 6526.
  3. N. Hongsith, C. Viriyaworasakul, P. Mangkorntong, N. Mangkorntong, S. Choopun, *Ceram Int* **34** (2008) 823.
  4. P. Gao, C. Lao, Y. Ding, Z. Wang, *Adv Funct Mater* **16** (2006) 53.
  5. S. Chen *et al.*, *J. Crys Growth* **240** (2002) 467.
  6. J.O. Cope, *Trans Faraday Soc* **67** (1961) 493.
  7. V. Noack, A. Eychmuller, *Chem Mater* **14** (2002) 1411.
  8. R. Devan *et al.*, *Nanoscale* **3** (2011) 4339.
  9. J. Lin *et al.*, *RSC Adv* **2** (2012) 2123.
  10. J. Lin *et al.*, *Sci Rep* **4** (2014) 6967.
  11. A. Rambu, N. Ifitimie, *Bull Mater Sci* **37** (2014) 441.
  12. S. Chen, Y. Liu, Y. Lu, J. Zhang, D. Shen, X. Fan, *J Crys Growth* **289** (2006) 55.
  13. A. Umar, Y.B. Hahn, *Crys Growth Des* **8** (2008) 2741.
  14. G. Exarhos, S. Sharma, *Thin Solid Films* **270** (1995) 27.